AD-A282 518

AD

TECHNICAL REPORT ARCCB-TR-94017

YIELD-BEFORE-BREAK FRACTURE MECHANICS ANALYSIS OF HIGH STRENGTH STEEL PRESSURE VESSELS

JOHN H. UNDERWOOD
RICHARD A. FARRARA
MICHAEL J. AUDINO

MAY 1994

US ARMY ARMAMENT RESEARCH,
DEVELOPMENT AND ENGINEERING CENTER
CLOSE COMBAT ARMAMENTS CENTER
BENÉT LABORATORIES
WATERVLIET, N.Y. 12189-4050

APPROVED FOR PUBLIC RELEASE; DISTRIBUTION UNLIMITED

DISCLAIMER

The findings in this report are not to be construed as an official Department of the Army position unless so designated by other authorized documents.

The use of trade name(s) and/or manufacturer(s) does not constitute an official indorsement or approval.

DESTRUCTION NOTICE

For classified documents, follow the procedures in DoD 5200.22-M, Industrial Security Manual, Section II-19 or DoD 5200.1-R, Information Security Program Regulation, Chapter IX.

For unclassified, limited documents, destroy by any method that will prevent disclosure of contents or reconstruction of the document.

For unclassified, unlimited documents, destroy when the report is no longer needed. Do not return it to the originator.

REPORT DOCUMENTATION PAGE

Form Approved
OMB No. 0704-0188

1. AGENCY USE ONLY (Leave blank)	2. REPORT DATE	3. REPORT TYPE AND DATES COVERED
	May 1994	Final

4. TITLE AND SUBTITLE
YIELD-BEFORE-BREAK FRACTURE MECHANICS ANALYSIS OF HIGH STRENGTH STEEL PRESSURE VESSELS

5. FUNDING NUMBERS
AMCMS: 611102H61111

6. AUTHOR(S)
John H. Underwood, Richard A. Farrara, and Michael J. Audino

7. PERFORMING ORGANIZATION NAME(S) AND ADDRESS(ES)
U.S. Army ARDEC
Benét Laboratories, SMCAR-CCB-TL
Watervliet, NY 12189-4050

8. PERFORMING ORGANIZATION REPORT NUMBER
ARCCB-TR-94017

9. SPONSORING/MONITORING AGENCY NAME(S) AND ADDRESS(ES)
U.S. Army ARDEC
Close Combat Armaments Center
Picatinny Arsenal, NJ 07806-5000

10. SPONSORING/MONITORING AGENCY REPORT NUMBER

11. SUPPLEMENTARY NOTES
Presented at the ASME Pressure Vessels and Piping Conference, Denver, Colorado, 26-29 July 1993. Published in the Conference Proceedings.

12a. DISTRIBUTION/AVAILABILITY STATEMENT
Approved for public release; distribution unlimited

12b. DISTRIBUTION CODE

13. ABSTRACT *(Maximum 200 words)*
Case study examples of fracture mechanics testing and analysis of Ni-Cr-Mo high strength steel cannon tubes are presented. The testing and analysis include significant plastic deformation accompanying fracture, which often occurs when high pressure is applied to high toughness steel pressure vessels. The analysis is based on a comparison of the size of the Irwin crack-tip plastic zone with the remaining ligament of the tube in the critical fatigue crack area that causes final failure. The results of the study show that the type of final failure can be predicted as either a relatively safe yield-before-break failure or a less safe running-crack type of failure for a variety of material, configuration, and loading conditions.

14. SUBJECT TERMS
Pressure Vessels, Fracture Mechanics, High Strength Steel, Plastic Yielding, Fatigue Failure

15. NUMBER OF PAGES
19

16. PRICE CODE

17. SECURITY CLASSIFICATION OF REPORT	18. SECURITY CLASSIFICATION OF THIS PAGE	19. SECURITY CLASSIFICATION OF ABSTRACT	20. LIMITATION OF ABSTRACT
UNCLASSIFIED	UNCLASSIFIED	UNCLASSIFIED	UL

NSN 7540-01-280-5500

Standard Form 298 (Rev 2-89)
Prescribed by ANSI Std Z39-18
298-102

TABLE OF CONTENTS

Tables

List of Illustrations

INTRODUCTION

Cyclic pressurization of a thick-walled cylinder will cause fatigue cracking if enough cycles of high pressure are applied. For cannon tubes, the pressure and number of firing cycles of the more severe service conditions are nearly always sufficient to cause fatigue cracking, therefore fatigue failure is always a possibility. The main concerns are the risk to life and the damage to materiel caused by the final, abrupt growth of the crack through the tube wall. There is a particular risk if this final growth through the wall is a large perforation, typically resulting in some amount of crack growth along the tube axis. This risk of final failure has been successfully addressed by testing several tubes to failure and using statistics to determine a safe firing life, which greatly minimizes the chance of any type of failure (ref 1). Although the use of a safe life reduces the risk of failure to an acceptable level, it has a cost--the significant difference between the conservative safe life and mean life from the fatigue tests. If a reliable description could be made of the severity of final failure of a cylinder, then a less conservative safe life could be used for a tube with a less severe type of failure, and there would be a significant cost savings associated with allowing the safe life to more closely approximate the mean life.

The objective of the work described in this report was to establish reliable criteria to distinguish between a severe final fatigue failure mode of a tube with considerable through-wall crack growth and a less severe mode with limited through-wall growth. Four series of cannon tube fatigue tests were analyzed to determine a simple, reliable description of the severity of the final fatigue failure. The ideal description would ensure a plastic yielding controlled failure and would be determined from easily obtained material properties and cylinder dimensions. In the following sections, a brief description of the fatigue tests and the applied stress intensity factor of the tests are given, and the concept of yield-before-break analysis of the final failure of the tubes is described.

Before proceeding with the yield-before-break discussions, the relationship of this topic with leak-before-break analysis of pressure vessels should be briefly discussed. The work of Schmitt et al. (ref 2) gives a good example of the leak-before-break concept as currently applied to pressure vessels, including the use of the J-integral concept to evaluate crack growth. Leak-before-break analysis is certainly useful to evaluate the failure of pressure vessels, but it addresses a point in the failure of a vessel beyond the scope of this work. Leak-before-break analysis evaluates the vessel after significant through-wall crack growth and associated leaking of the pressure vessel have occurred. Yield-before-break analysis evaluates the point where the crack is still a part-through surface crack in order to describe the severity of the final failure about to occur. In addition, the yield-before-break method is typically applied to higher strength, lower toughness steels than the leak-before-break method.

FATIGUE TESTS

Hydraulic fatigue tests have been performed at the U.S. Army Armament Research, Development, & Engineering Center for a variety of Ni-Cr-Mo high strength steel cannon tubes. The test procedures and results for 175-mm inner diameter (ID) tubes are described in Reference 1. Similar tests for three other size tubes have been performed, as listed in Table 1. The tubes have radius ratio, r_2/r_1, of about 2, tensile strength of 1100 to 1400 MPa, and a composition typical of ASTM A723 steel. Details are given in Table 1. The 155-, 105-, and 120-mm tubes were overstrained before testing and had a residual stress distribution corresponding to plastic deformation through about 60 percent of the wall thickness. The details of the residual stresses are discussed later. The 175-mm tubes had no intentionally-produced residual stress.

The fatigue tests were performed by hydraulic pressurization of cylinders typically 1 m long with inner and outer radii, as given in Table 1, and pressure, P, as listed in Table 2. Figure 1 is a sketch of the test specimen and some of the nomenclature. Note that the semi-elliptical-shaped surface crack from the ID surface in the sketch is typical of most, but not all, of the tests here. As discussed later, four of the six 155-mm tubes had surface cracks that grew from a notch on the outer diameter (OD) surface. The critical depth, a_{cr} and length, $2c_{cr}$ of the crack at the point of final failure are listed in Table 2 as crack depth and crack shape ratios. The fracture toughness, K_{Icr} and yield strength, S_y, of the tube material were measured and are listed in Table 2. For the 175-mm tube material, the standard ASTM K_{Ic} method could be used because of the relatively low toughness and high yield strength. For the other materials, a J_{Ic} test method was used (ref 3), and a critical stress intensity factor, K_J, was calculated from J_{Ic}.

APPLIED STRESS INTENSITY FACTOR

Any useful description of the severity of the final failure of pressurized tubes should involve the applied stress intensity factor, K_{apl}, the fundamental driving force for a crack. At the least, it should be shown that

$$K_{apl} \geq K_{Ic} \tag{1}$$

for the final failure to occur. A general expression for K_{apl} for a pressurized, overstrained, thick-walled tube can be written as follows:

$$K_{apl} = 1.12(S_p + S_r + P)(\pi a/Q)^{1/2} \tag{2}$$

Equation (2) is an expression for ID or OD surface cracks of depth "a" and shape factor Q in the same form as that of Newman and Raju (ref 4), who also gave a simple form of Q as

$$Q = 1 + 1.464(a/c)^{1.65} \tag{3}$$

The factor 1.12 in Eq. (2) is from the K solution for a shallow edge crack. The factor $(1/Q)^{1/2}$ varies from 1.00 for a straight-fronted crack (a/c = 0) to 0.64 for a semicircular crack (a/c = 1); this reduction in K_{apl} by as much as a factor of 0.64 accounts for the lower applied K for a semi-elliptical crack compared with the K for a straight-fronted crack.

The $(S_p + S_r + P)$ term in Eq. (2) is made up of the following. The circumferential stress, S_p, due to pressure, P, at any radius, r, in the tube wall is the familiar Lamé stress (ref 5)

$$S_p = P[(r_2/r)^2 + 1]/[(r_2/r_1)^2 - 1] \tag{4}$$

The circumferential residual stress, S_r, at any radius equal to or larger than the plastic radius, ρ, is (ref 6)

$$S_r = S_{YS}[(r_2/r)^2 + 1][(\rho^2/2r_2^2) + (r_1^2/(r_2^2 - r_1^2))((\rho^2 - r_2^2)/2r_2^2 - \ln(\rho/r_1))] \qquad (5)$$

Finally, the pressure, P, is included in the stress term of Eq. (2) when there is pressure applied to the crack faces, typically for ID-initiated cracks. For OD cracks, P is not included in Eq. (2). Combining Eqs. (2) through (5) gives the expression for the applied K for the deepest point of a surface crack in a pressurized and overstrained cylinder, with the condition that the radial position of the crack tip is (r_1 + 0.6 t) or greater. This condition is met for all tests here, except for the 175-mm tubes, for which $S_R = 0$ and Eq. (5) does not apply. Equations (2) through (5) are expected to give accurate values for relatively shallow cracks, a/t → 0, since the expressions converge to accurate limit solutions for shallow cracks. For deeper cracks, there is no generally applicable limit solution available, so the accuracy of the calculated K_{apl} is less certain. However, the equations account for the factors known to be important for a surface-cracked cylinder--the applied and residual stresses in the wall, the pressure in the crack, and the effect of crack shape--in a rational and consistent manner. The results should provide at least a useful comparison among the various tests.

The K_{apl} values from Eqs. (2) through (5) (with r set equal to the radial position of the crack tip) for each of the eighteen cylinder tests are listed in Table 2 and plotted in Figure 2 versus K_{Ic}. The plot shows a dashed line corresponding to $K_{apl} = K_{Ic}$. Note that all results are above this line and that cylinders with relatively low K_{Ic} and correspondingly shallow critical crack depths are closer to the $K_{apl} = K_{Ic}$ line. This is consistent with the expectations of accuracy discussed in the preceding paragraph. Another check on the K_{apl} results from Eqs. (2) through (5) can be made by a comparison with the recent results of Kendall and Perez (ref 7), who calculated K for a pressurized tube in a similar but more comprehensive manner than that used here. Their results included crack configurations, which allowed a direct comparison with three of the four crack configurations of the 175-mm tubes, as shown in Figure 2. They are from 10 to 20 percent above the values from Eqs. (2) through (5), which is in reasonably good agreement. The significantly higher K_{apl} values compared to K_{Ic} noted in Figure 2 have been observed by other investigators for similar conditions. The work of Jones and Brown (ref 8) could explain at least some of the elevation of K_{apl} relative to K_{Ic} in the results here. They found a progressive increase in the critical K for fracture of a 1470 MPa yield strength 4340 steel, as the specimen thickness decreased. Their results, repeated here in Figure 3, were part of the basis for the specimen size requirements for K_{Ic} tests now widely accepted. Clark (ref 9) investigated the effect on measured K_{Ic} of the K level of fatigue precracking preceding the K_{Ic} test. For a Ni-Cr-Mo steel with 1100 MPa yield strength, he found a K_{Ic} of 110 MPa√m when the fatigue K level was 55 MPa√m or lower and an apparent K_{Ic} of 152 MPa√m when the fatigue K level was about 150 MPa√m. This type of significant increase in apparent K_{Ic} could have been present in the fatigue tests here, because the fatigue K level just before final failure was inherently close to the K at final failure. Reuter and Epstein (ref 10) observed critical surface crack K values at fracture that were up to twice the K_{Ic} value of the titanium alloy investigated. They suggested that a loss of plane-strain constraint at the point where the surface crack intersected the free surface caused K_{apl} to be greater than K_{Ic}.

The experience of other investigators (refs 8-10) and the results herein suggest the following regarding the high K_{apl} at fracture relative to K_{Ic}. The small remaining ligament in the specimen certainly contributed to the high K_{apl} in the same fundamental way as the specimen thickness effect described by Jones and Brown and the free surface effect discussed by Reuter and Epstein. Also, the fatigue K level effect discussed by Clark probably added to the increase of K_{apl} at fracture. Regardless of the specific cause of the high K_{apl} relative to K_{Ic}, this basic result shows that one required condition for final failure of the cylinders has been met--that the applied K must at least equal the material fracture toughness, K_{Ic}. The next task is to describe and predict, if possible, the nature of the final failure.

YIELD-BEFORE-BREAK ANALYSIS

The tube fatigue tests showed two locations of failure, one in Figure 4(a) where the dominant fatigue crack grew from the ID and finally broke through to the OD, and one in Figure 4(b) where the crack grew from an OD notch and broke through to the ID. As previously mentioned, important features of the final failure were the remaining uncracked ligament in the tube wall ahead of the crack of critical depth, the dimension b_c, and the axial length of break-through of the crack, the dimension $2c_f$, both shown in Figure 4. These dimensions are believed to be important in describing the nature of the final failure.

Irwin Plastic Zone

The size of b_c relative to the crack-tip plastic zone size, r_y, may control the final failure of the tube in the same way that the specimen thickness relative to r_y affects the critical K in a fracture toughness test (ref 8), as discussed earlier. The now classic work by Irwin (ref 11) gave expressions for the crack-tip plastic zone and used them to develop failure criteria for various engineering applications, including pressure vessels. Following Irwin's approach, an expression for the plane-strain plastic zone is

$$r_y = [1/6\pi][K_{Ic}/S_{YS}]^2 \qquad (6)$$

and a proposed criterion for separating between the small plastic zone case, where elastic stresses control fracture, and the large plastic zone case, where plastic deformation controls, is the following:

$$b_c = \beta[K_{Ic}/S_{YS}]^2 \qquad (7)$$

In Eq. (7), β is a constant expected to be near 2.5, the familiar value used for separation between the small plastic zone case of plane-strain fracture toughness tests (ref 12) and the large plastic zone, the plane-stress case discussed earlier. In prior work (ref 13), Eq. (7) was used with $\beta = 2.5$ to distinguish between different types of failure behavior of cylinders using the K_{Ic} test experience (ref 12) as a basis. Table 3 lists the measured b_c at failure, the ratio $\beta = b_c/[K_{Ic}/S_y]^2$, and the type of final failure for each tube test. A running-crack failure was indicated when the through-wall length of crack after failure was greater than the surface length of crack just before failure, that is, $c_f/c_c > 1$. Note that the nine running-crack failures of 175-, 155-, and 120-mm tubes would have been predicted by Eq. (7), since $\beta > 2.5$, but one additional 120-mm running-crack failure would have been predicted that, in fact, did not occur.

A plot of the results and concepts discussed above is shown in Figure 5. The line $b_c = [K_{Ic}/S_y]^2$ is shown, which corresponds to $\beta = 1$. Note that this line effectively separates the tube tests that show a running-crack from those which do not. For $b_c \leq [K_{Ic}/S_y]^2$, there is enough plastic yielding at the crack tip to control the final failure and prevent the dangerous running-crack behavior. This criterion is referred to here as the yield-before-break condition,

$$b_c \leq [K_{Ic}/S_{YS}]^2 \tag{8}$$

the critical size of the remaining ligament below which a safe, plastic deformation controlled final failure can be expected for a pressurized tube with a surface crack. The fundamental requirement for yield-before-break in a tube is a plastic zone large enough relative to the remaining ligament that crack-tip blunting or stress relaxation occurs and prevents the running-crack. There was one case, mentioned earlier, for which the predictions of Eq. (8) did not match the tube test results: 120-mm tube #14 had a $\beta = 1.7$, which was > 1 and yet did not show a running-crack. Note, however, that the ratio c_f/c_c for #14 was the highest value of any test that showed yielding behavior.

Axial Cracking Accompanying Failure

The amount of axial cracking that occurs as a result of final failure, $2c_f$, is worth further consideration, because it is easily characterized and it is directly related to the severity of the failure. The amount of post-failure axial cracking relative to the pre-failure surface crack length, c_f/c_c (from Table 3), is compared to the relative ligament size of the yield-before-break criterion, as shown in Figure 6. Although there is some scatter, there is a clear linear relationship between c_f/c_c and $b_c/[K_{Ic}/S_y]^2$, as indicated by the linear regression line. This relationship shows a direct link between a useful measure of the severity of failure, c_f, and key configurational and material properties associated with the failure, b_c, K_{Ic} and S_y. This gives support to the use of the yield-before-break criterion for describing and predicting the severity of the final fatigue failure of pressurized tubes. For example, note in Figure 6 that the tubes which meet the yield-before-break criterion are in a clearly separate group and that this group also forms a separate group in which $c_f/c_c < 1$. The 120-mm tube #14 previously mentioned is an exception here as well, but the trend is clear: yield-before-break failures with $b_c \leq [K_{Ic}/S_y]^2$ also result in relatively small amounts of axial cracking, that is, $c_f/c_c \leq 1$.

Yield-Before-Break in Design

The tube results can be used to demonstrate the use of the yield-before-break criterion in design. Imagine the case of a pressurized tube of some given size that had a remaining ligament at a failure of 13 mm, which is the average b_c in Table 3. Then, using the K_{Ic} and S_y values of Table 2, a design plot can be made, as shown in Figure 7. For tubes with these K_{Ic} and S_y properties and loading such that b_c = 13 mm, the use of a yield strength much above 1200 MPa will result in a running-crack type of failure. The designer could change the loading or configuration of the tube to decrease b_c, but a far more effective way of assuring yield-before-break is to increase the $[K_{Ic}/S_y]$ ratio. This is true because the $[K_{Ic}/S_y]$ quantity is squared and also because of the interrelation of K_{Ic} and S_y--when S_y is decreased, K_{Ic} is significantly increased for nearly all materials. Therefore, small decreases in S_y cause large decreases in $b_c/[K_{Ic}/S_y]^2$ and in the severity of the failure expected. This can be clearly seen in the trend line in Figure 7. If only K_{Ic} were increased while S_y were held constant, the decrease in $b_c/[K_{Ic}/S_y]^2$ and the associated decrease in failure severity would not be nearly as pronounced as that shown in Figure 7. Other penalties associated with increasing K_{Ic} with S_y constant are increased material cost and decreased availability.

SUMMARY

The key findings and conclusions of this study are the following:

1. A yield-before-break criterion for pressurized, surface-cracked, high strength steel tubes has been developed following the approach of the Irwin plastic zone concept. For conditions where the remaining ligament at failure is small relative to the ligament required for plane-strain conditions, a yield-before-break failure is expected. In equation form, the criterion is

$$b_c \le [K_{Ic}/S_{YS}]^2$$

2. Failure conditions for eighteen A723 steel tubes showed that when the yield-before-break criteria was met, the length of the dangerous through-wall axial crack accompanying failure was consistently small compared to the critical surface crack length just before fracture. This observation, that $c_f/c_c \le 1$, provides direct quantitative support to the yield-before-break concept.

3. The most effective way to obtain a yield-before-break condition in pressure vessel design is by using the minimum possible yield strength consistent with design requirements, because this changes each of the three key parameters in the yield-before-break criterion in the proper way: a reduction in b_c, a reduction in $(S_y)^2$, and an increase in $(K_{Ic})^2$.

REFERENCES

1. T.E. Davidson, J.F. Throop, and J.H. Underwood, "Failure of a 175-mm Cannon Tube and the Resolution of the Problem Using an Autofrettaged Design," *Case Studies in Fracture Mechanics*, AMMRC MS 77-5, Army Materials and Mechanics Research Center, Watertown, MA, 1977, pp. 3.9.1- 3.9.13.

2. W. Schmitt, G. Nagel, A. Ockewitz, L. Hodulak, and J.G. Blauel, "Analytical and Numerical Crack Growth Prediction for a Leak-Before-Break Assessment of a Nuclear Pressure Vessel," *International Journal of Pressure Vessels and Piping*, Vol. 43, 1990, pp. 255-271.

3. J.H. Underwood, E.J. Troiano, and R.T. Abbott, "Simpler J_{Ic} Test and Data Analysis Procedures for High Strength Steels," *Fracture Mechanics: Twenty-Fourth Symposium, ASTM STP 1207*, American Society for Testing and Materials, Philadelphia, 1994.

4. J.C. Newman, Jr. and I.S. Raju, "An Empirical Stress-Intensity Factor Equation for the Surface Crack," *Engineering Fracture Mechanics*, Vol. 15, 1981, pp. 185-192.

5. R.J. Roark and W.C. Young, *Formulas for Stress and Strain*, McGraw-Hill, New York, 1975, p. 504.

6. T.E. Davidson, D.P. Kendall, and A.N. Reiner, "Residual Stresses in Thick-Walled Cylinders Resulting from Mechanically-Induced Overstrain," *Experimental Mechanics*, November 1963, pp. 253-262.

7. D.P. Kendall and E.H. Perez, "Comparison of Stress Intensity Factor Solutions for Thick-Walled Pressure Vessels," *Proceedings of 1993 ASME Pressure Vessel and Piping Conference, High Pressure - Codes, Analysis, and Applications*, PVP Vol. 263 (Ashe Khare, Ed.), 1993, p. 115.

8. M.H. Jones and W.F. Brown, Jr., "The Influence of Crack Length and Thickness in Plane Strain Fracture Toughness Tests," *Review of Developments in Plane Strain Fracture Toughness Testing, ASTM STP 463*, American Society for Testing and Materials, Philadelphia, 1970, pp. 63-101.

9. G. Clark, "Significance of Fatigue Stress Intensity in Fracture Toughness Testing," *International Journal of Fracture*, Vol. 15, 1979, pp. R179-R181.

10. W.G. Reuter and J.S. Epstein, "Experimental Evaluation of an Equation Applicable for Surface Cracks Under Tensile or Bending Loads," *Fracture Mechanics: Nineteenth Symposium, ASTM STP 969*, (T.A. Cruse, Ed.), American Society for Testing and Materials, Philadelphia, 1988, pp. 597-619.

11. G.R. Irwin, "Structural Aspects of Brittle Fracture," *Applied Materials Research*, Vol. 3, 1964, pp. 65-81.

12. "E-399 Standard Test Method for Plane-Strain Fracture Toughness of Metallic Materials," *Annual Book of ASTM Standards*, Vol. 03.01, American Society for Testing and Materials, Philadelphia, 1992, pp. 506-536.

13. J.H. Underwood and B.B. Brown, "Analysis of Leak-Before-Break Failures of Thick-Wall Steel Pressure Vessels with Surface Fatigue Cracks," *Proceedings of SEM Conference on Experimental Mechanics*, Keystone, CO, November 1986.

Table 1. Tube Size and Radius Ratio, Material Characteristics

Cylinder		Tensile Strength MPa	Material Designation -	Measured Chemical Composition Weight Percent					
$2r_1$ mm	r_2/r_1 -			C	Ni	Cr	Mo	V	S
175	2.13	1390	4335V	0.36	1.79	1.16	0.68	0.14	0.008
155	1.79	1320	A723	0.33	2.22	0.94	0.40	0.10	0.013
105	1.90	1090	A723	0.34	3.19	0.87	0.67	0.23	0.008
120	2.25	1180	A273	0.33	3.07	1.10	0.54	0.13	0.003

Table 2. Fracture Toughness, Yield Strength, Crack Dimensions, and Loading Conditions

Tube	Fracture Toughness at 20°C K_{Ic} or K_J MPa$\sqrt{m}$	Yield Strength at 20°C S_{YS} MPa	Crack Dimensions and Applied Loads			
			Crack Depth a_o/t -	Crack Shape $a_o/2C_e$ -	Applied Pressure P MPa	Applied K K_{apl} MPa$\sqrt{m}$
175-mm #31	142	1256	0.43	0.10	345	251
#63	103	1270	0.43	0.41	377	201
#82	108	1277	0.38	0.36	377	204
#86	117	1249	0.46	0.30	377	231
155-mm #1	134	1187	0.31	0.05	393	181
#2	187	1221	0.83	0.26	393	374
#3	152	1207	0.87	0.27	393	373
#5	151	1228	0.28	0.07	393	169
#9	135	1248	0.31	0.10	393	179
#11	113	1242	0.26	0.06	393	164
105-mm #38	164	1007	0.83	0.18	380	319
#51	165	994	0.87	0.23	380	306
#66	152	1056	0.79	0.22	414	327
#71	162	1014	0.70	0.12	414	346
120-mm #6	152	1173	0.65	0.26	669	515
#14	155	1152	0.60	0.26	669	500
#23	185	1125	0.85	0.18	669	587
#85	188	1056	0.93	0.30	669	519

Table 3. Yield-Before-Break Calculations and Results

Tube	Ligament at Failure b_c mm	Constant in Eq. (7) $b_c/[K_{Ic}/S_{YS}]^2$	Nature of Final Failure		
			Location	Type	c_f/c_c
175 mm #31	56	4.4	ID	Running	1.73
#63	56	8.5	ID	Running	7.10
#82	61	8.5	ID	Running	7.04
#86	53	6.0	ID	Running	4.88
155 mm #1	42	3.3	OD	Running	1.42
#2	10	0.4	ID	Yield	0.41
#3	8	0.5	ID	Yield	0.46
#5	44	2.9	OD	Running	2.22
#9	42	3.6	OD	Running	2.78
#11	45	5.4	OD	Running	2.06
105 mm #38	8	0.3	ID	Yield	0.06
#51	6	0.2	ID	Yield	0.18
#66	10	0.5	ID	Yield	0.21
#71	14	0.5	ID	Yield	0.25
120 mm #6	26	1.5	ID	Running	1.79
#14	30	1.7	ID	Yield	0.88
#23	11	0.4	ID	Yield	0.34
#85	5	0.2	ID	Yield	0.11

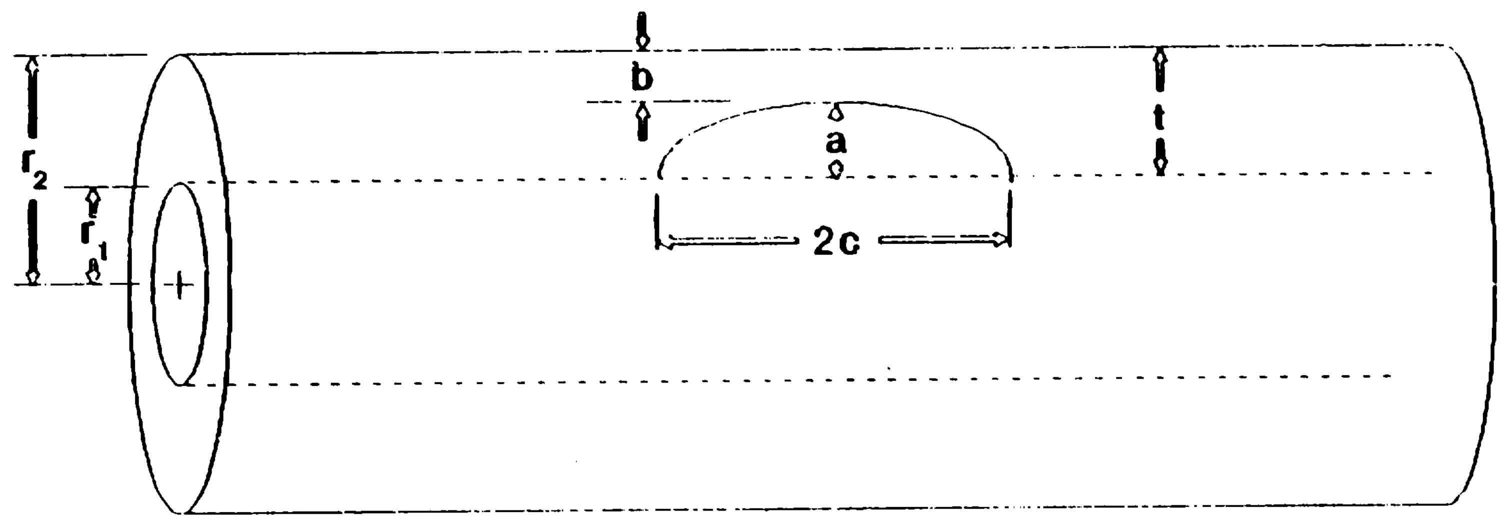

Figure 1
Tube and crack configuration
and nomenclature

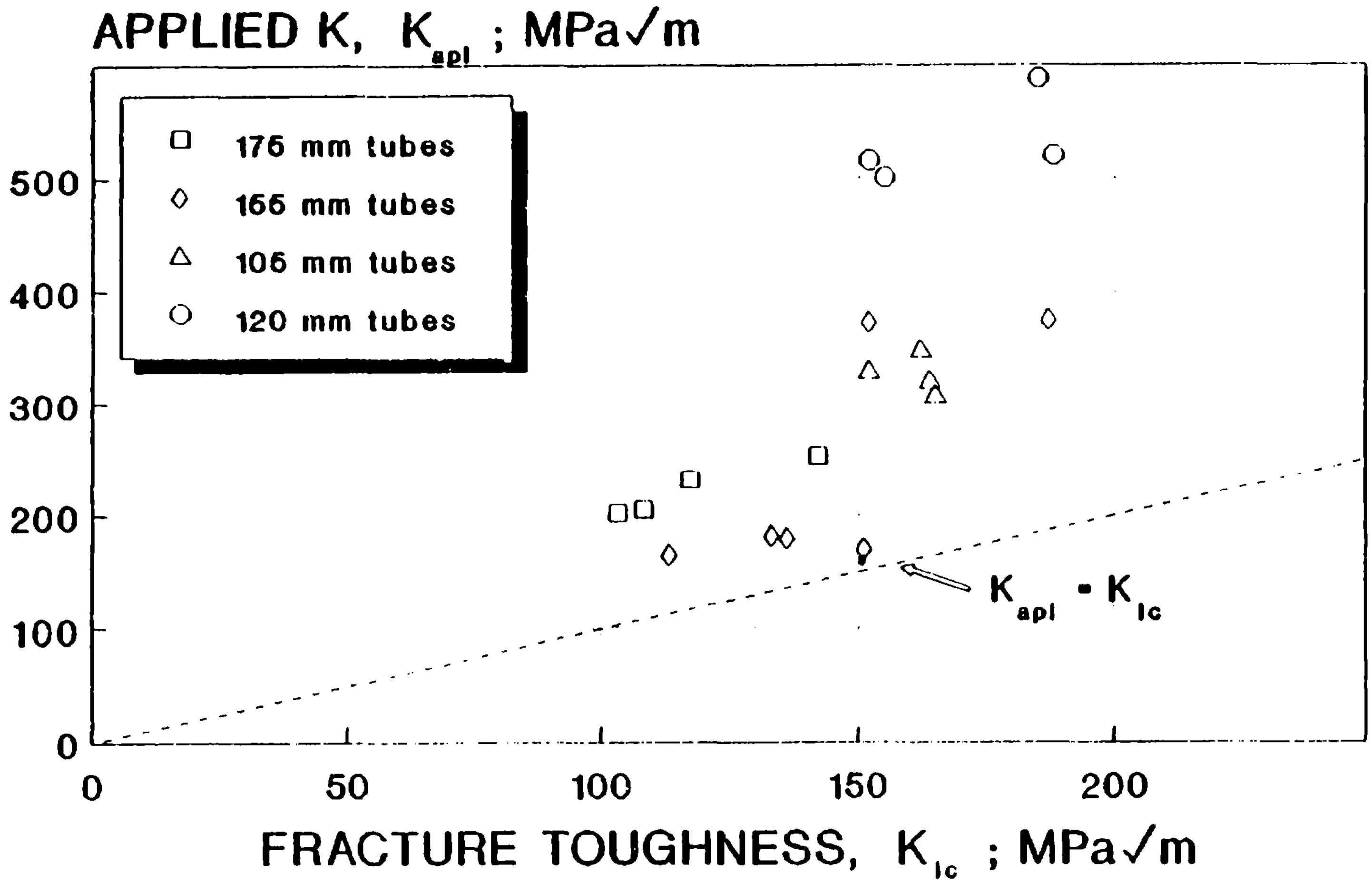

Figure 2
Comparison of applied K with material fracture toughness, K_{Ic}

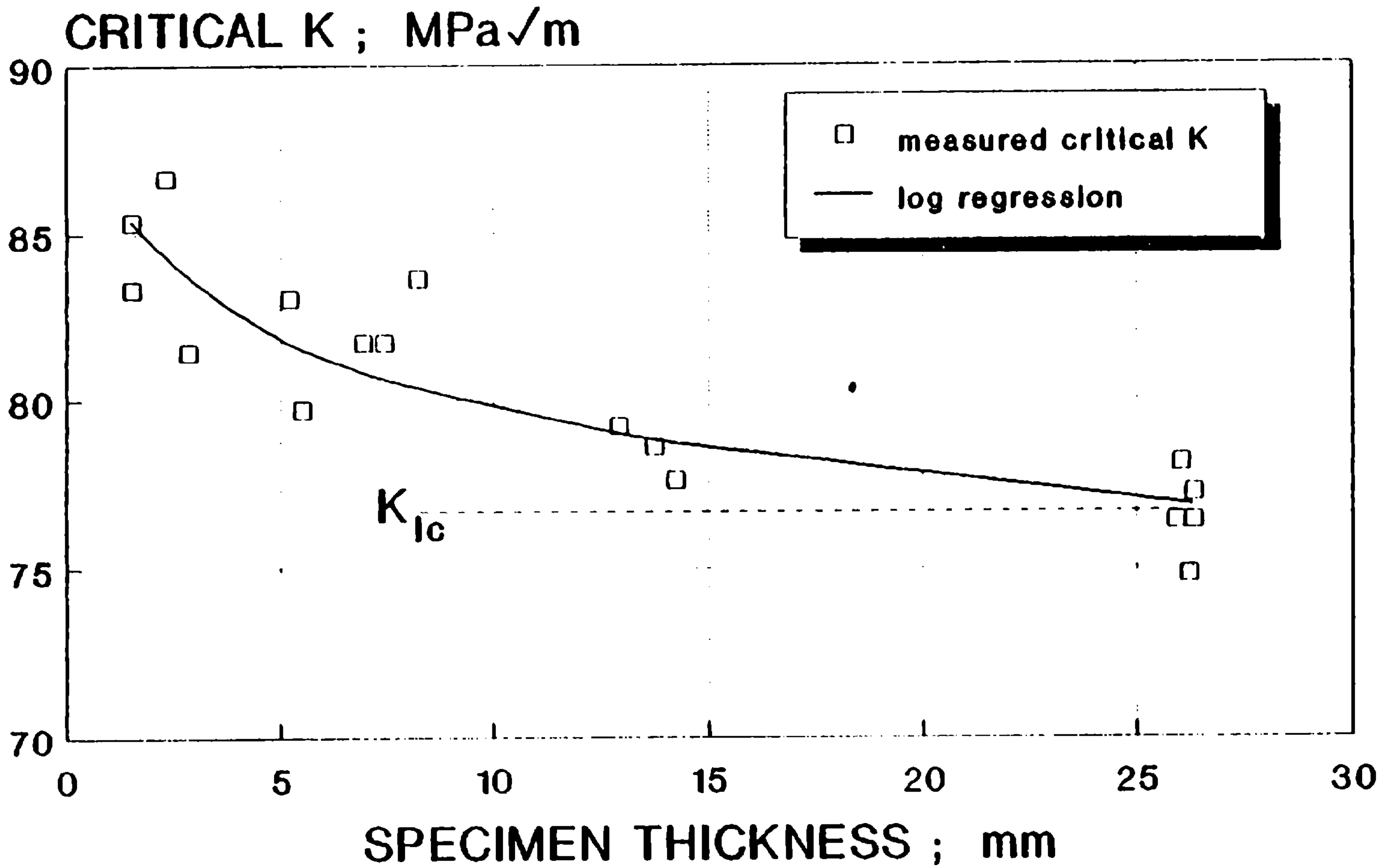

Figure 3
Effect of specimen size on critical K
for crack extension in 4340 steel

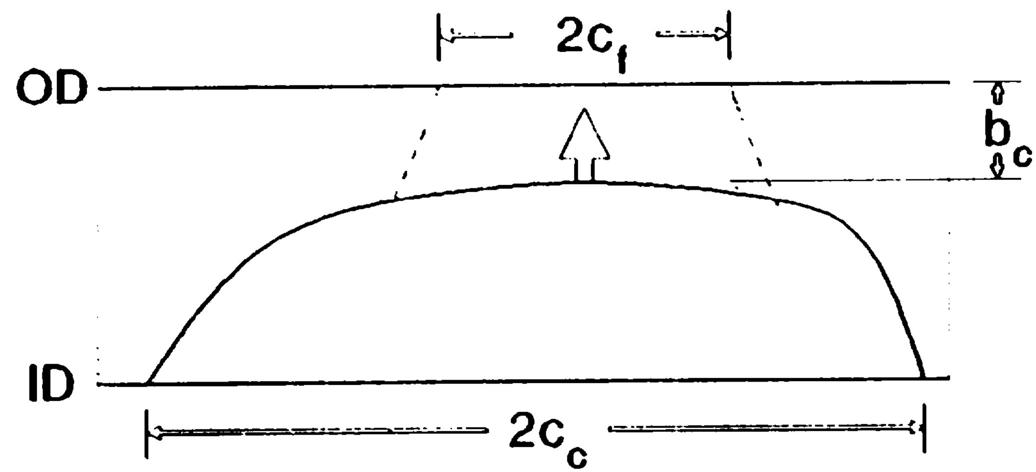

[a] Cracking from the ID

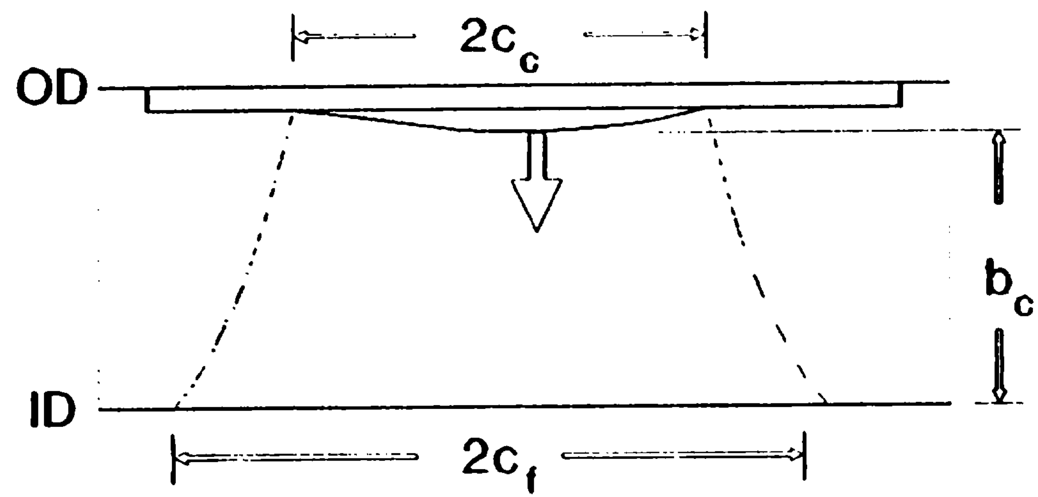

[b] Cracking from a notch on the OD

Figure 4
Types of final failure observed in fatigue loaded thick-wall cylinders

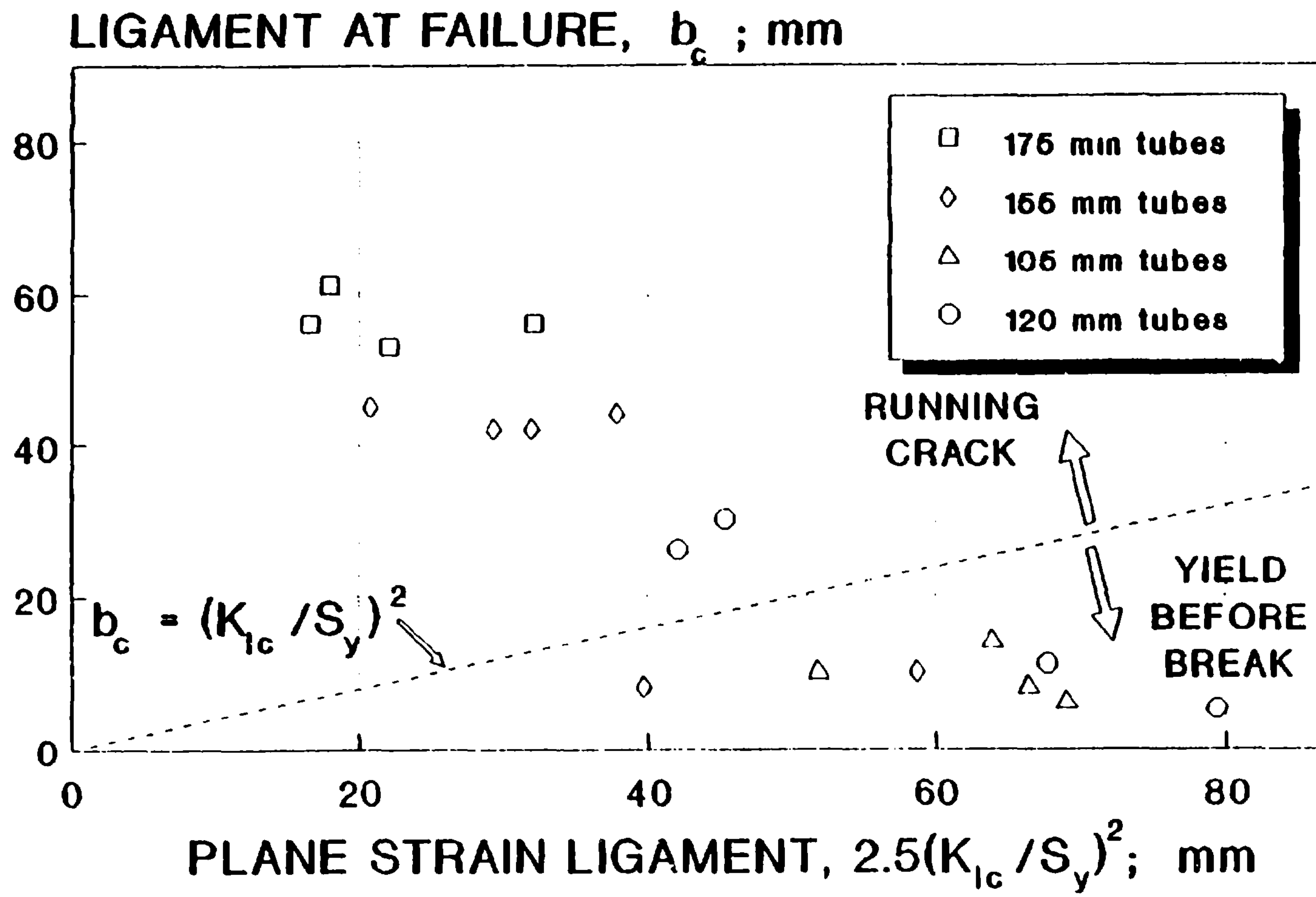

Figure 5
Plane–strain ligament size compared with remaining ligament at failure

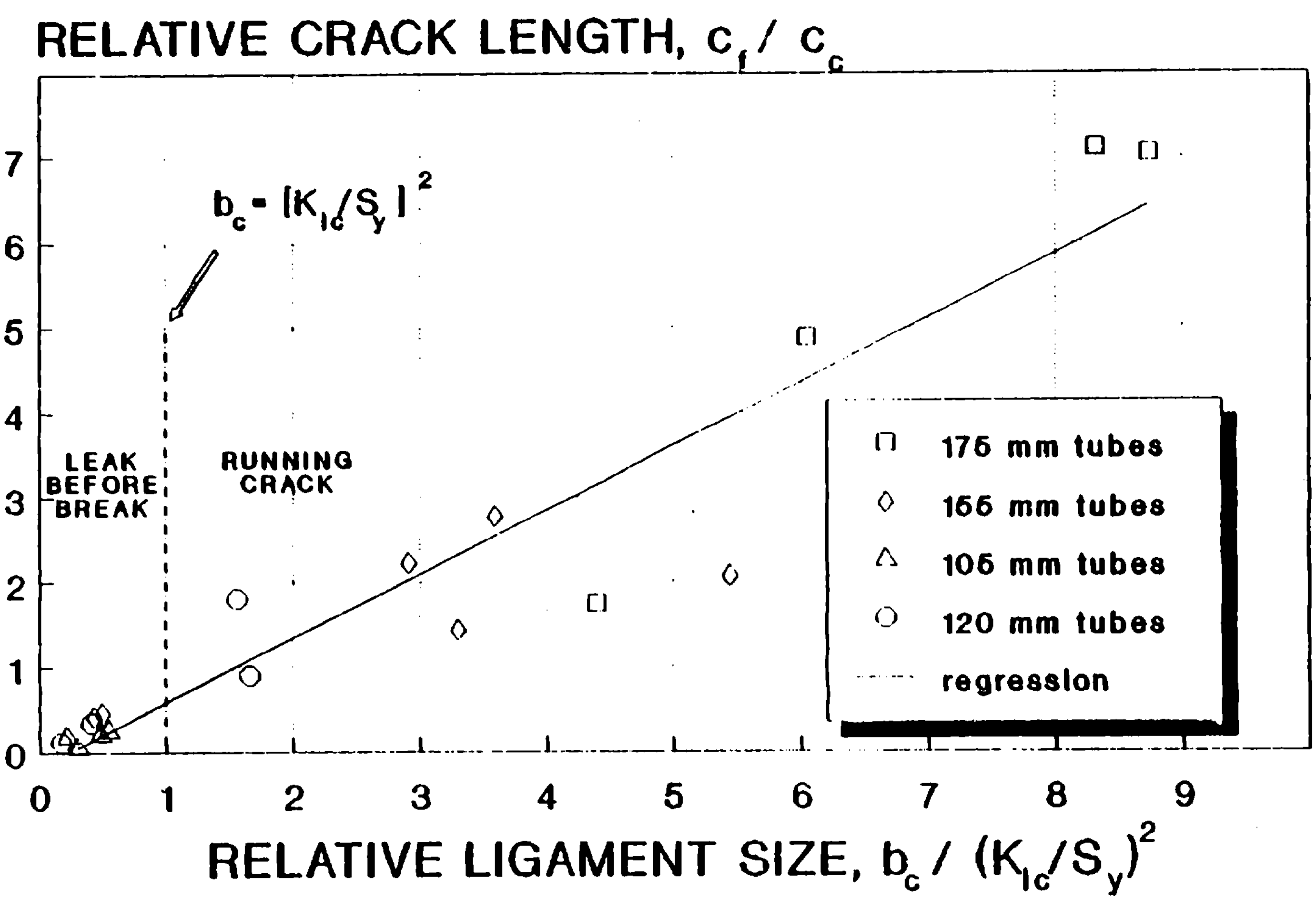

Figure 6
Effect of critical ligament size on axial crack length after failure

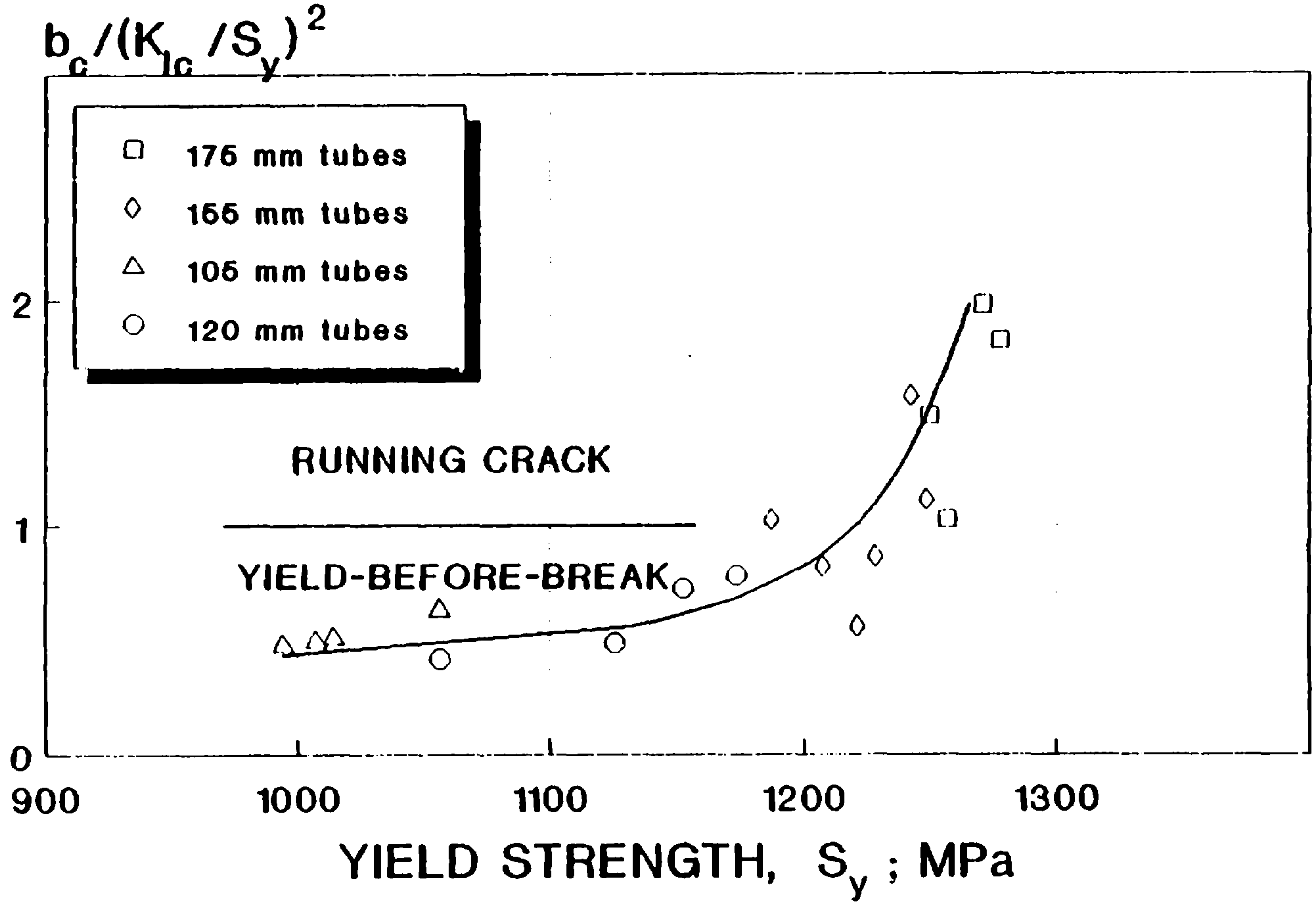

Figure 7
Effect of material yield strength
on severity of final failure

TECHNICAL REPORT INTERNAL DISTRIBUTION LIST

	NO. OF COPIES
CHIEF, DEVELOPMENT ENGINEERING DIVISION	
ATTN: SMCAR-CCB-DA	1
-DC	1
-DI	1
-DR	1
-DS (SYSTEMS)	1
CHIEF, ENGINEERING DIVISION	
ATTN: SMCAR-CCB-S	1
-SD	1
-SE	1
CHIEF, RESEARCH DIVISION	
ATTN: SMCAR-CCB-R	2
-RA	1
-RE	1
-RM	1
-RP	1
-RT	1
TECHNICAL LIBRARY	
ATTN: SMCAR-CCB-TL	5
TECHNICAL PUBLICATIONS & EDITING SECTION	
ATTN: SMCAR-CCB-TL	3
OPERATIONS DIRECTORATE	
ATTN: SMCWV-ODP-P	1
DIRECTOR, PROCUREMENT & CONTRACTING DIRECTORATE	
ATTN: SMCWV-PP	1
DIRECTOR, PRODUCT ASSURANCE & TEST DIRECTORATE	
ATTN: SMCWV-QA	1

NOTE: PLEASE NOTIFY DIRECTOR, BENÉT LABORATORIES, ATTN: SMCAR-CCB-TL OF ADDRESS CHANGES.

TECHNICAL REPORT EXTERNAL DISTRIBUTION LIST

	NO. OF COPIES
ASST SEC OF THE ARMY	
RESEARCH AND DEVELOPMENT	
ATTN: DEPT FOR SCI AND TECH	1
THE PENTAGON	
WASHINGTON, D.C. 20310-0103	
ADMINISTRATOR	
DEFENSE TECHNICAL INFO CENTER	12
ATTN: DTIC-FDAC	
CAMERON STATION	
ALEXANDRIA, VA 22304-6145	
COMMANDER	
U.S. ARMY ARDEC	
ATTN: SMCAR-AEE	1
SMCAR-AES, BLDG. 321	1
SMCAR-AET-O, BLDG. 351N	1
SMCAR-CC	1
SMCAR-FSA	1
SMCAR-FSM-E	1
SMCAR-FSS-D, BLDG. 94	1
SMCAR-IMI-I, (STINFO) BLDG. 59	2
PICATINNY ARSENAL, NJ 07806-5000	
DIRECTOR	
U.S. ARMY RESEARCH LABORATORY	
ATTN: AMSRL-DD-T, BLDG. 305	1
ABERDEEN PROVING GROUND, MD 21005-5066	
DIRECTOR	
U.S. ARMY RESEARCH LABORATORY	
ATTN: AMSRL-WT-PD (DR. B. BURNS)	1
ABERDEEN PROVING GROUND, MD 21005-5066	
DIRECTOR	
U.S. MATERIEL SYSTEMS ANALYSIS ACTV	
ATTN: AMXSY-MP	1
ABERDEEN PROVING GROUND, MD 21005-5071	

	NO. OF COPIES
COMMANDER	
ROCK ISLAND ARSENAL	
ATTN: SMCRI-ENM	1
ROCK ISLAND, IL 61299-5000	
MIAC/CINDAS	
PURDUE UNIVERSITY	
P.O. BOX 2634	1
WEST LAFAYETTE, IN 47906	
COMMANDER	
U.S. ARMY TANK-AUTMV R&D COMMAND	
ATTN: AMSTA-DDL (TECH LIBRARY)	1
WARREN, MI 48397-5000	
COMMANDER	
U.S. MILITARY ACADEMY	
ATTN: DEPARTMENT OF MECHANICS	1
WEST POINT, NY 10966-1792	
U.S. ARMY MISSILE COMMAND	
REDSTONE SCIENTIFIC INFO CENTER	2
ATTN: DOCUMENTS SECTION, BLDG. 4484	
REDSTONE ARSENAL, AL 35898-5241	
COMMANDER	
U.S. ARMY FOREIGN SCI & TECH CENTER	
ATTN: DRXST-SD	1
220 7TH STREET, N.E.	
CHARLOTTESVILLE, VA 22901	
COMMANDER	
U.S. ARMY LABCOM	
MATERIALS TECHNOLOGY LABORATORY	
ATTN: SLCMT-IML (TECH LIBRARY)	2
WATERTOWN, MA 02172-0001	
COMMANDER	
U.S. ARMY LABCOM, ISA	
ATTN: SLCIS-IM-TL	1
2800 POWER MILL ROAD	
ADELPHI, MD 20783-1145	

NOTE: PLEASE NOTIFY COMMANDER, ARMAMENT RESEARCH, DEVELOPMENT, AND ENGINEERING CENTER, U.S. ARMY AMCCOM, ATTN: BENET LABORATORIES, SMCAR-CCB-TL, WATERVLIET, NY 12189-4050 OF ADDRESS CHANGES.

TECHNICAL REPORT EXTERNAL DISTRIBUTION LIST (CONT'D)

	NO. OF COPIES
COMMANDER U.S. ARMY RESEARCH OFFICE ATTN: CHIEF, IPO P.O. BOX 12211 RESEARCH TRIANGLE PARK, NC 27709-2211	 1
DIRECTOR U.S. NAVAL RESEARCH LABORATORY ATTN: MATERIALS SCI & TECH DIV CODE 26-27 (DOC LIBRARY) WASHINGTON, D.C. 20375	 1 1
COMMANDER AIR FORCE ARMAMENT LABORATORY ATTN: AFATL/MN EGLIN AFB, FL 32542-5434	 1
COMMANDER AIR FORCE ARMAMENT LABORATORY ATTN: AFATL/MNF EGLIN AFB, FL 32542-5434	 1

NOTE: PLEASE NOTIFY COMMANDER, ARMAMENT RESEARCH, DEVELOPMENT, AND ENGINEERING CENTER, U.S. ARMY AMCCOM, ATTN: BENÉT LABORATORIES, SMCAR-CCB-TL, WATERVLIET, NY 12189-4050 OF ADDRESS CHANGES.

END

FILMED

DATE: 8-94

DTIC